Analysing Superimposed Oriented Patterns

Ingo Stuke, Til Aach
Institute for Signal Processing,
University of Lübeck,
Ratzeburger Allee 160,
D-23538 Lübeck, Germany
{stuke,aach}@isip.uni-luebeck.de

Erhardt Barth, Cicero Mota
Institute for Neuro- and Bioinformatics,
University of Lübeck
Ratzeburger Allee 160,
D-23538 Lübeck, Germany
{barth,mota}@inb.uni-luebeck.de

Abstract

Estimation of local orientation in images is often posed as the task of finding the minimum variance axis in a local neighborhood. The solution is given as the eigenvector belonging to the smaller eigenvalue of a 2×2 tensor. Ideally, the tensor is rank-deficient, i.e., the smaller eigenvalue is zero. A large minimal eigenvalue signals the presence of more than one local orientation. We describe a framework for estimating such superimposed orientations. Our analysis of superimposed orientations is based on the eigensystem analysis of a suitably extended tensor. We show how to efficiently carry out the eigensystem analysis using tensor invariants. Unlike in the single orientation case, the eigensystem analysis does not directly yield the orientations, rather, it provides so-called mixed orientation parameters. We therefore show how to decompose the mixed orientation parameters into the individual orientations. These, in turn, allow to separate the superimposed patterns.

1. Introduction

Analysis of local orientation in an image is an essential step in, e.g., directional filtering [1, 2], directional interpolation [8], feature extraction, tracking, motion estimation [12, 11, 9, 5] and pattern analysis [7, 10, 5]. Multiple orientations appear in non-opaque imagery like X-ray, ultrasound, and Computer Tomography and in image features like corners, crossings and bifurcations. Here we present an approach for estimating multiple orientations for additively overlaid patterns. The solution is based on earlier results for multiple transparent motions [13, 12]. Orientation estimation for two superimposed patterns is expressed as the eigensystem analysis of a generalized structure tensor. Unlike in the single-orientation case, the tensor concept now leads to a nonlinear problem that is here linearized by introducing so-called *mixed-orientation parameters*. The mixed-orientation parameters form a unique descriptor of double-orientation neighborhoods, but do not provide the orientations explicitly. Decomposing the mixed-orientation parameters into the individual orientations is solved by seeking the intersections of a line and a circle. Furthermore, we derive a hierarchical algorithm which allows to deal with single and superimposed orientations.

Work supported by Deutsche Forschungsgemeinschaft under Ba 1176/7-2

2. Single orientation estimation

A two-dimensional image $f(\mathbf{x}), \mathbf{x} = (x, y)$ is oriented in a region Ω if

$$f(\mathbf{x}) = f(\mathbf{x} + \mathbf{u}) \tag{1}$$

$\forall\, \mathbf{x}, \mathbf{x} + \mathbf{u} \in \Omega$. The vector $\mathbf{u} = (\cos\theta, \sin\theta)^T$ describes the orientation of $f(\mathbf{x})$ in terms of the angle θ, which is conventionally restricted to lie in the interval $(-\pi/2, \pi/2]$. In order to estimate the local orientation, we follow the differential approach introduced in [6, 5, 10, 4], which finds the minimum gray level variance axis within the local neighborhood Ω. Let

$$\alpha(\phi) = \cos(\phi)\frac{\partial}{\partial x} + \sin(\phi)\frac{\partial}{\partial y} \tag{2}$$

denote the derivative operator with respect to the vector $(\cos\phi, \sin\phi)^T$. Unless $f(\mathbf{x})$ is locally constant, it has an unique orientation θ at $\mathbf{x}$ if and only if its directional derivative in the direction of θ vanishes, i.e.

$$\begin{aligned} \alpha(\theta) f(\mathbf{x}) &= \cos(\theta) f_x(\mathbf{x}) + \sin(\theta) f_y(\mathbf{x}) \\ &= \mathbf{u}^T \nabla f(\mathbf{x}) = 0 \end{aligned} \tag{3}$$

In practice, local orientation is estimated within a local neighborhood Ω by minimizing the residual

$$\varepsilon(\mathbf{u}) = \int_{\Omega} \left(\mathbf{u}^T \nabla f(\mathbf{x})\right)^2 \mathbf{d}\Omega = \mathbf{u}^T \mathbf{J}_1 \mathbf{u}, \text{ s.t. } \mathbf{u}^T\mathbf{u} = 1 \tag{4}$$

with respect to $\mathbf{u}$. The constraint $\mathbf{u}^T\mathbf{u} = 1$ excludes the trivial solution $\mathbf{u} = 0$. The symmetric 2×2-tensor $\mathbf{J}_1$ is

$$\mathbf{J}_1 = \int_{\Omega} (\nabla f)(\nabla f)^T \mathbf{d}\Omega = \int_{\Omega} \begin{bmatrix} f_x^2 & f_x f_y \\ f_x f_y & f_y^2 \end{bmatrix} \mathbf{d}\Omega. \tag{5}$$

Minimization of the composite criterion

$$E(\mathbf{u}) = \mathbf{u}^T \mathbf{J}_1 \mathbf{u} + \lambda(1 - \mathbf{u}^T\mathbf{u}) \tag{6}$$

with λ being an arbitrary constant, is equivalent to

$$\mathbf{J}_1\mathbf{u} = \lambda\mathbf{u} \text{ s.t. } \mathbf{u}^T\mathbf{u} = 1. \tag{7}$$

The solution $\mathbf{u}$ is then the eigenvector of $\mathbf{J}_1$ corresponding to its smallest eigenvalue λ_2. The minimum residual is equal to this smallest eigenvalue, i.e. $\varepsilon(\mathbf{u}) = \lambda_2$. Eq. (4) evidently assumes that only a single orientation is present within Ω. Compliance with this assumption is indicated by a low value of λ_2, and a high value for the larger eigenvalue λ_1. Indeed, if the single-orientation hypothesis is ideally met, the residual λ_2 is zero, and hence, rank$(\mathbf{J}_1) = 1$. Violation of the single-orientation hypothesis is indicated by a large residual λ_2. This in turn indicates that more than one oriented structure is present in Ω. In the following, we will show how multiple superimposed orientations can be locally estimated.

3. Estimation of two overlaid orientations

We model a double-oriented pattern by $f(\mathbf{x}) = g_1(\mathbf{x}) + g_2(\mathbf{x})$. Since the two components g_1 and g_2 are assumed to be ideally oriented in the directions θ and γ, respectively, they satisfy the following equations

$$\alpha(\theta) g_1 = \mathbf{u}^T \nabla g_1 = 0 \quad \alpha(\gamma) g_2 = \mathbf{v}^T \nabla g_2 = 0 \tag{8}$$

where $\mathbf{u} = (\cos\theta, \sin\theta)^T$ and $\mathbf{v} = (\cos\gamma, \sin\gamma)^T$. Therefore, the composite image $f(\mathbf{x})$ satisfies (for multiple motions the analog equations have been derived in [13])

$$\begin{aligned} &\alpha(\theta)\alpha(\gamma) f = \\ &\quad \big(\cos(\theta)\frac{\partial}{\partial x} + \sin(\theta)\frac{\partial}{\partial y}\big)\big(\cos(\gamma)\frac{\partial}{\partial x} + \sin(\gamma)\frac{\partial}{\partial y}\big) f \\ &\quad = \mathbf{c}^T \mathbf{d} f = 0 \end{aligned} \tag{9}$$

where

$$\mathbf{c} = (\cos(\theta)\cos(\gamma), \sin(\theta+\gamma), \sin(\theta)\sin(\gamma))^T \tag{10}$$

and

$$\mathbf{d}f = (f_{xx}, f_{xy}, f_{yy})^T. \tag{11}$$

The vector $\mathbf{c}$ is the result of the concatenation of two directional derivative operators, and thus combines both orientations θ and γ. We will refer to $\mathbf{c}$ as the mixed-orientation vector. Let $F(\omega)$ denote the Fourier transform of $f(\mathbf{x})$ over Ω. We then obtain in the Fourier domain

$$\alpha(\theta)\alpha(\gamma) f(\mathbf{x}) = 0 \;\circ\!\!-\!\!\bullet\; (\mathbf{u}^T\omega)(\mathbf{v}^T\omega) F(\omega) = 0, \tag{12}$$

where ω is the frequency vector. The above equation implies that the local spectrum $F(\omega)$ must be zero except for the lines $\mathbf{u}^T\omega = 0$ and $\mathbf{v}^T\omega = 0$. The non-zero spectral components at $\mathbf{u}^T\omega = 0$ correspond to the Fourier transform of $g_1(\mathbf{x})$ and those at $\mathbf{v}^T\omega = 0$ to the transform of $g_2(\mathbf{x})$. Consequently, for $\omega = 0$ the frequency components of both layers are superimposed. Eq. (8) and Eq. (12) ensure that Eq. (9) is a necessary and sufficient condition for the existence of a double orientation as long as Eq. (9) is evaluated within a region Ω. As in the single-orientation case, the residual error ε_2 of Eq. (9) within Ω is defined as

$$\varepsilon_2(\mathbf{c}) = \mathbf{c}^T \mathbf{J}_2 \mathbf{c} \tag{13}$$

where

$$\begin{aligned} \mathbf{J}_2 &= \int_{\Omega} (\mathbf{d}f)(\mathbf{d}f)^T d\Omega \\ &= \int_{\Omega} \begin{bmatrix} f_{xx}^2 & f_{xx}f_{xy} & f_{xx}f_{yy} \\ f_{xx}f_{xy} & f_{xy}^2 & f_{xy}f_{yy} \\ f_{xx}f_{yy} & f_{xy}f_{yy} & f_{yy}^2 \end{bmatrix} d\Omega. \end{aligned} \tag{14}$$

Minimizing ε_2 with respect to $\mathbf{c}$ under the constraint $\mathbf{c}^T\mathbf{c} = 1$, we obtain $\mathbf{c}$ as the eigenvector of the 3×3 tensor $\mathbf{J}_2$ that corresponds to the smallest eigenvalue λ_3. The minimum residual error is then equal to λ_3. Confidence for the double-orientation hypothesis is high if λ_3 is small and the other eigenvalues are large. The resulting mixed-orientation vector $\mathbf{c}$ is an unambiguous descriptor of double orientation neighborhoods, which could be used as, e.g., tracking feature. It does, however, not yet explicitly provide the orientations.

3.1. Decomposing the mixed-orientation vector

The eigenvector analysis of the generalized tensor $\mathbf{J}_2$ in Eq. (13) defines the vector $\mathbf{c}$ only up to an unknown scaling factor R, i.e.

$$\begin{aligned} \mathbf{c} &= R\,(\cos(\theta)\cos(\gamma), \sin(\theta+\gamma), \sin(\theta)\sin(\gamma))^T \\ &= (a, b, c)^T. \end{aligned} \tag{15}$$

Though R is unknown, it complies with the constraint $\mathbf{c}^T\mathbf{c} = 1$, i.e., $a^2 + b^2 + c^2 = 1$. We first observe that

$$a \mp c = R\cos(\theta \pm \gamma), \quad b = R\sin(\theta+\gamma) \tag{16}$$

These expressions cannot be inverted to find $\theta+\gamma$ and $\theta-\gamma$ because, even though θ and γ are restricted to lie within $(-\pi/2, \pi/2]$, we have $-\pi < \theta \pm \gamma \leq \pi$. The inversion of the cosine and sine functions is, however, ambiguous in this interval.

An alternative solution, similar to solutions derived for multiple motions, consists of seeking the roots of a polynomial constructed from the components a, b, and c of the mixed-orientation vector, see [12, 3]. We use

$$\begin{aligned} \frac{b}{a} &= \frac{\sin(\theta+\gamma)}{\cos(\theta)\cos(\gamma)} = \tan(\theta)+\tan(\gamma), \\ \frac{c}{a} &= \frac{\sin(\theta)\sin(\gamma)}{\cos(\theta)\cos(\gamma)} = \tan(\theta)\cdot\tan(\gamma) \end{aligned} \tag{17}$$

as coefficients to construct the polynomial

$$P(z) = z^2 - \frac{b}{a}z + \frac{c}{a} = (z-\tan\theta)\,(z-\tan\gamma) \tag{18}$$

We could then determine $\tan(\theta)$ and $\tan(\gamma)$ as roots of $P(z)$. The angles could therefore be unambiguously obtained within $(-\pi/2, \pi/2]$. We would, however, have to deal with the singularity at $a=0$ in cases where $\theta=\pi/2$ or $\gamma=\pi/2$.

Starting from the above result, we now show a solution that avoids these difficulties. We propose a decomposition method that determines the auxiliary vectors $\mathbf{P} = (\cos(2\theta), \sin(2\theta))$ and $\mathbf{Q} = (\cos(2\gamma), \sin(2\gamma))$ as the intersections of a line with the unit circle. To do so, we first replace the variable z of $P(z)$ by one of the roots of $P(z)$, here denoted by y/x where the ratio is either defined by $x=\cos\theta$ and $y=\sin\theta$ in case of $\mathbf{P}$ or $x=\cos\gamma$ and $y=\sin\gamma$ for $\mathbf{Q}$. Eq. (18) then becomes equivalent to

$$cx^2 - bxy + ay^2 = 0. \tag{19}$$

Now we observe that

$$\begin{aligned} x^2 &= \cos^2\theta = \frac{1}{2} + \frac{1}{2}\cos 2\theta, \\ y^2 &= \sin^2\theta = \frac{1}{2} - \frac{1}{2}\cos 2\theta, \\ xy &= \sin\theta\cos\theta = \frac{1}{2}\sin 2\theta. \end{aligned} \tag{20}$$

Note that analog equations are valid for γ. Therefore, the two points $\mathbf{P} = (\cos 2\theta, \sin 2\theta)$ and $\mathbf{Q} = (\cos 2\gamma, \sin 2\gamma)$ lie on the line

$$mX + nY - r = 0, \tag{21}$$

where X and Y are the first and second components of $\mathbf{P}$ and $\mathbf{Q}$, respectively. The parameters m, n, r are

$$m = \frac{a-c}{\sqrt{1-2ac}},\; n = \frac{b}{\sqrt{1-2ac}},\; r = \frac{a+c}{\sqrt{1-2ac}} \tag{22}$$

where m, n, and r are normalized to satisfy $m^2+n^2=1$. From Eq. (21) and the additional constraint $\mathbf{c}^T\mathbf{c}=1$ (see above) we can draw the following two conclusions: (i) $1-2ac$ is always positive and (ii) the points $\mathbf{P}$ and $\mathbf{Q}$ are given as the intersections of the line defined by Eq. (21) and the unit circle. Note that the vector $\mathbf{e}_1 = (m, n)$ is orthogonal and $\mathbf{e}_2 = (-n, m)$ is parallel to the line. Since r is the distance between the line and the origin, the points $\mathbf{P}$ and $\mathbf{Q}$ are found by the linear combination

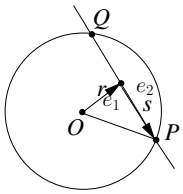

Figure 1. Geometry of the separation.

$$\mathbf{P}, \mathbf{Q} = r\mathbf{e}_1 \mp s\mathbf{e}_2 \tag{23}$$

where $s = \sqrt{1-r^2}$. Figure 1 depicts the geometric interpretation of the separation procedure. Finally, $\mathbf{P}$ and $\mathbf{Q}$ determine the orientations.

4. Confidence measures

As we have seen, orientation estimation is ideally only possible if the structure tensors $\mathbf{J}_1$ or $\mathbf{J}_2$ have a single zero eigenvalue. As shown in [12], the above confidence criterion can be expressed in terms of the tensor-invariants without explicit evaluation of the eigenvalues. Such a confidence criterion is especially useful for 2×2 and 3×3 matrices because its evaluation based on the minors of the tensor is simpler and faster. The tensor $\mathbf{J}_1$ has the invariants:

$$\begin{aligned} K_1 &= \det\mathbf{J}_1 = \lambda_1\,\lambda_2 \\ &= \langle f_x^2\rangle\langle f_y^2\rangle - \langle f_x f_y\rangle^2 \\ H_1 &= \text{trace}\mathbf{J}_1 = \lambda_1+\lambda_2 = \langle f_x^2\rangle + \langle f_y^2\rangle, \end{aligned} \tag{24}$$

where $\langle f_x^2\rangle = \int_\Omega f_x^2 \mathbf{d}\Omega$, and so on. Clearly, $H_1 = 0$ if and only if $\lambda_1 = \lambda_2 = 0$. This can only occur in homogeneous regions where no orientations can be estimated. In case of single orientations the confidence criterion translates to $H_1 > 0$ and $K_1 = 0$. As shown in [12], these invariants obey $K_1 \leq H_1^2$. Equality holds for isotropic regions only, i.e., $H_1 = K_1 = 0$. Thus the confidence criterion becomes $K_1 \leq \epsilon_1 H_1^2$ with a confidence parameter ϵ_1.

In regions where the single-orientation model is rejected by the above confidence criterion, we test for the double-orientation model. For tensor $\mathbf{J}_2$ we use the invariants

$$\begin{aligned} K_2 &= \det(\mathbf{J}_2) = \lambda_1\lambda_2\lambda_3 = \langle f_{xx}^2\rangle M_{33} \\ &- \langle f_{xx} f_{xy}\rangle M_{32} + \langle f_{xx} f_{yy}\rangle M_{31} \\ S_2 &= (\lambda_1\lambda_2 + \lambda_1\lambda_3 + \lambda_2\lambda_3) \\ &= M_{11} + M_{22} + M_{33}, \end{aligned} \tag{25}$$

where M_{ij} are the minors obtained from $\mathbf{J}_2$ by eliminating row $4-i$ and column $4-j$. In analogy to the single-orientation case, we obtain the confidence criterion $K_2^2 \leq \epsilon_2 S_2^3$. As shown in [12], for any matrix having a single zero eigenvalue the eigenvector corresponding to the zero eigenvalue can be expressed in terms of the minors. For $\mathbf{J}_1$ this eigenvector is

$$\begin{aligned} \mathbf{u} &= \frac{(-\langle f_x f_y\rangle, \langle f_x^2\rangle)^T}{\sqrt{\langle f_x^2\rangle^2 + \langle f_x f_y\rangle^2}} \quad \text{or} \\ \mathbf{u} &= \frac{(\langle f_y^2\rangle, -\langle f_x f_y\rangle)^T}{\sqrt{\langle f_y^2\rangle^2 + \langle f_x f_y\rangle^2}} \end{aligned} \tag{26}$$

For $\mathbf{J}_2$ there are three possibilities to compute the eigenvector corresponding to the zero eigenvalue:

$$\mathbf{c}_i = R_i(M_{i3}, -M_{i2}, M_{i1})^T = (a_i, b_i, c_i)^T,\ i = 1,2,3 \tag{27}$$

where the scaling factors R_i are not needed in our analysis, but can be determined by $(a_i + c_i)^2 + b_i^2 = R_i^2$ according to Eq. (16).

5. Layer separation

For some applications it is useful to separate the superimposed patterns using the double-orientation information. Let $g_1(\mathbf{x})$ and $g_2(\mathbf{x})$ be oriented in directions θ and γ, respectively. The directional derivative $\alpha(\theta)f(\mathbf{x})$ nulls out $g_1(\mathbf{x})$ (see Eq. (8)), and yields in the Fourier domain

$$\alpha(\theta)f(\mathbf{x}) = \alpha(\theta)g_2(\mathbf{x}) \circ\!\!-\!\!\bullet\, \omega^T\, \mathbf{u} G_2(\omega) =: \bar{G}_2(\omega). \tag{28}$$

The pattern $g_2(\mathbf{x})$ is thus recovered up to a convolution. At frequencies where $\omega^T\, \mathbf{u} \neq 0$ we obtain $G_2(\omega)$ by

$$G_2(\omega) = \frac{\bar{G}_2(\omega)}{\omega^T\, \mathbf{u}}. \tag{29}$$

The frequencies where $\omega^T\, \mathbf{u} = 0$ correspond to the support of $G_1(\omega)$ and therefore

$$G_2(\omega^T\, \mathbf{u}) = 0. \tag{30}$$

Since both lines (determined by $\mathbf{u}$ and $\mathbf{v}$ respectively) pass through the origin, it is impossible to separate the frequency components at the origin. Accordingly, the mean values of the patterns cannot be recovered.

6. Results

Figure 2 shows two sinusoidal patterns that are superimposed: one is vertically oriented and the other is a section of a circle. We added Gaussian white noise with an SNR of 25dB. The estimated orientation vectors are depicted in the right image (15-fold sub-sampling). For each pattern

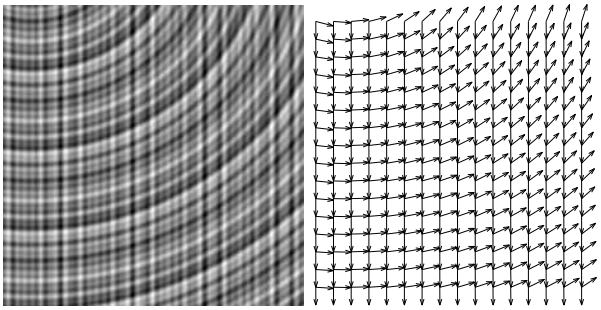

Figure 2. Two overlaid patterns.

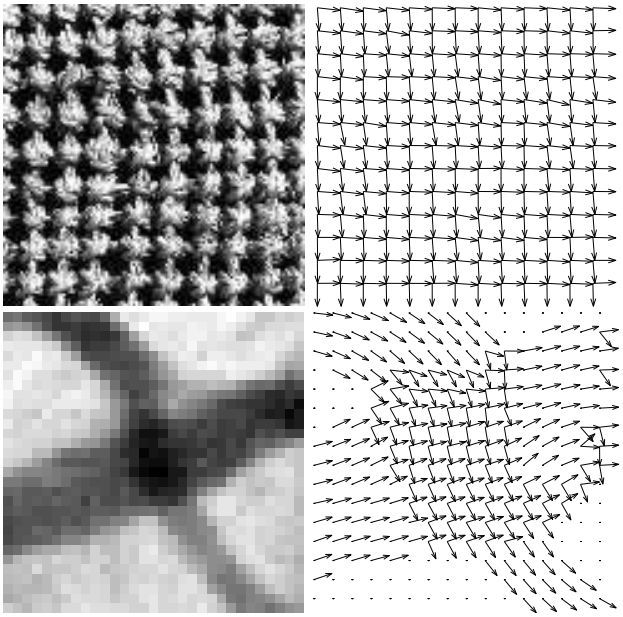

Figure 3. Results for fabric with two opaque orientations (top) and an X-rayed blood vessel crossing (bottom).

we performed an error analysis by comparing the estimates with the known ground truth. For the vertical oriented pattern the mean squared angular error is 0.28 degrees and its standard deviation 0.29 degrees. For the circular pattern, the errors are estimated relative to the tangent, and we observed an MSE of 1.48 and a STD of 0.94 degrees. The parameters ϵ_1 and ϵ_2 are set to 0.1 and 0.4 respectively, and the size of the integration area Ω was 7×7 pixels. The top left image in Figure 3 depicts a fabric, which was taken from the MIT-VisTex database. The estimated orientations are shown top right for every tenth pixel. Even though the image does not satisfy the superposition assumption, the estimated orientations correspond well to the orientations in the texture. The parameters ϵ_1 and ϵ_2 are set to 0.2 and 0.6, respec-

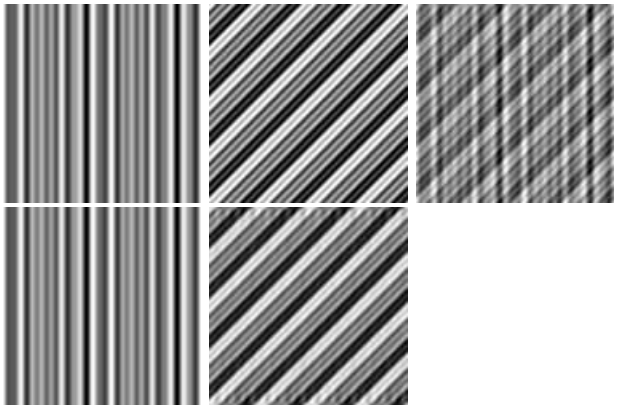

Figure 4. Layer Separation

tively, and the size of the integration area is 21×21 pixels. The second example of figure 3 shows a small part of an X-ray image with a blood vessel crossing. In this case the superposition is approximately additive. The estimated orientations are depicted on the right image. Note that in the overlapping region the two orientations are quite accurately detected. For the non-overlaid vessel parts the single orientation is also accurately estimated. We used a integration filter size of 9×9 pixels and the parameters $\epsilon_1 = 0.6$ and $\epsilon_2 = 0.6$. In all three examples we used a Gaussian pre-filter with size 3×3 pixels and standard deviation of one pixel. Derivatives were computed by finite differences. Figure 4 shows an example for layer separation. The first row depicts the two original layers (top left and middle) and their overlay (top right). In the second row we show the separated layers. We were able to recover the layers except for their mean values.

7. Conclusions

We presented methods for the detection, estimation, and separation of two locally overlaid orientations in images. A key element is a generalized structure tensor that is defined for any number of orientations. We have used this tensor to first detect the number of orientations based on confidence measures that do not involve an eigenvalue analysis. Instead, these measures can be fast and efficiently calculated by the invariants of the generalized structure tensor, which in turn are calculated in terms of the tensor minors. The overlaid orientations are unambiguously described by a mixed-orientation vector, which is given as the tensor's eigenvector corresponding to the smallest (ideally zero) eigenvalue. As for the confidence measures, we have shown that the mixed-orientation vector can be calculated from the tensor minors without an explicit eigensystem analysis. It is a powerful feature of local image content, and uniquely decomposable into the individual orientations. Finally, we have used the orientation parameters to separate the overlaid image patterns. Our results, for real and synthetic images, illustrate the potential of our framework. The orientation parameters are quite accurately recovered under noisy conditions and a wide range of relative orientations. Test patterns were well separated into the original layers. Further examples illustrate the benefit for texture analysis and vessel segmentation.

References

[1] T. Aach, D. Kunz. Anisotropic spectral magnitude estimation filters for noise reduction and image enhancement. *Proc. IEEE Int. Conf. Im. Proc.*:335–8, Lausanne, Sept. 16–19, 1996.

[2] T. Aach, D. Kunz. A lapped directional transform for spectral image analysis and its application to restoration and enhancement. *Signal Processing*, 80:2347–64, 2000.

[3] E. Barth, I. Stuke, C. Mota. Analysis of motion and curvature in image sequences. *Proc. IEEE Southwest Symp. Im. Anal. Interp.*:206–10, Santa Fe, NM, Apr. 7–9, 2002.

[4] J. Bigün, G. H. Granlund. Optimal orientation detection of linear symmetry. *IEEE 1st Intl. Conf. Comp. Vis.*:433–8, London, June 1987.

[5] J. Bigün, G. H. Granlund, J. Wiklund. Multidimensional orientation estimation with application to texture analysis and optical flow. *IEEE T PAMI*, 13(8):775–90, 1991.

[6] S. Di Zenzo. A note on the gradient of a multi-image. *Comp. Vis. Graph. Im. Proc.*, 33:116–25, Jan. 1986.

[7] W. T. Freeman, E. H. Adelson. The design and use of steerable filters. *IEEE T PAMI*, 13(9):891–906, 1991.

[8] J. Hladuvka, E. Gröller. Direction-driven shape-based interpolation of volume data. T. Ertl et.al. (eds.), *Proc. Vis. Model. Visualiz.*:113–20, Stuttgart, Nov. 21–23, 2001. Aka GmbH.

[9] B. Jähne. Image sequence analysis in environmental and life sciences. B. Michaelis, G. Krell (eds), *Patt. Recog., 25th DAGM Symp., Lect. Notes Comp. Scie.*, vol. 2781:608–17, Magdeburg, Sept. 10–12, 2003. Springer.

[10] M. Kass. W. Witkin. Analyzing oriented patterns. *Comp. Vis. Graph. Im. Proc.*, 37:362–85, 1987.

[11] R. Mester. Some steps towards a unified motion estimation procedure. In *Proc. 45th IEEE MidWest Symp. Circ. Syst.*, Tulsa, OK, Aug. 4–7, 2002.

[12] C. Mota, I. Stuke, E. Barth. Analytic solutions for multiple motions. In *Proc. IEEE Int. Conf. Im. Proc.*, vol. II: 917–20, Thessaloniki, Oct. 7–10, 2001.

[13] M. Shizawa, K. Mase. Simultaneous multiple optical flow estimation. In *IEEE Conf. Comp. Vis. Patt. Recog.*, vol. I:274–8, Atlantic City, NJ, June 1990.